2010 11th. Int. Conf. Control, Automation, Robotics and Vision
Singapore, 5-8th December 2010

Urban Vehicle Platoon using Monocular Vision: Scale Factor Estimation

P. Avanzini[1,3], B. Thuilot[1,3] and P. Martinet[2,3]
[1] Clermont Université, Université Blaise Pascal, LASMEA, BP 10448, 63000 Clermont-Ferrand, France
[2] Clermont Université, IFMA, LASMEA, BP 10448, 63000 Clermont-Ferrand, France
[3] CNRS, UMR 6602, LASMEA, 63177 Aubière, France
Pierre.AVANZINI@lasmea.univ-bpclermont.fr

***Abstract*—Environment, sustainable development as well as new transportation service emergence in urban areas are major concerns. Consequently, studies are currently intended to automate electric vehicles designed for applications in free access. An additional functionality that appears very attractive is vehicle platooning. In order to avoid oscillations within the fleet when completing this task, a global control strategy, supported by inter-vehicle communications, is investigated. Vehicle absolute localization is then needed and is here derived from monocular vision. These data are however expressed in a virtual vision world, slightly distorted with respect to the actual metric one. It has previously been shown that such a distortion can accurately be corrected on-line in different ways, considering telemetric or odometric data. These strategies have here been refined in order to provide optimal corrections. A comparative study, supported by simulations and full-scale experiments, is reported to exhibit benefits and performances of proposed approaches.**

***Index Terms*—automatic guided vehicles, platooning, nonlinear control, monocular vision, urban vehicles**

I. Introduction

Nowadays the development of new transportation systems is essential to fulfill the increasing requirements in terms of service and ecology. These needs, which all the more manifest themselves in urban environment, are concretized by the use of electric vehicles in free access. In this context, autonomous navigation constitutes a very attractive solution. More coherent motion could furthermore be achieved by considering cooperating vehicles, thus increasing safety and efficiency. Vehicle platooning moreover allows to easily adapt the transport offer (via platoon length) to the actual need, and can also ease maintenance operations, since only one person can then move several vehicles at a time (e.g. to bring them back to some station). Platooning is therefore considered in this paper.

Different approaches can be proposed. They can be classified into two categories, according to the information used for vehicle control. The most standard approaches rely on ***local strategies***, i.e. each vehicle is controlled exclusively from data relative to the neighboring vehicles. The well-known *leader-follower approach* considers only the immediate front vehicle. For instance, visual tracking has been proposed in [3] and generic control laws have been designed in [12] and [6]. Alternatively, neighboring vehicles (and not only the preceding one) are taken into account when using *virtual structure approaches*: a structural analogy, characterized by a serial chain of spring-damper, is for instance proposed in [13] and a control law is then derived from the combined front and rear virtual forces.

These strategies present however some drawbacks, the most concerning one being error accumulation: the servoing errors, induced by sensor noises and/or actuator delays, are inevitably growing from the first vehicle to the last one, leading to unacceptable oscillations. Such problems can be overcome by considering ***global strategies***, i.e. each vehicle is now controlled from the data received from all vehicles. Most of the *virtual structure approaches* belong to this category. In [5], a mechanical analogy is used to design feedback controllers to achieve straight line motion. A single virtual rigid structure is also considered in [7], relying on graph theory. Nevertheless, these techniques aim at imposing some pre-specified geometric pattern, and not that each vehicle accurately reproduces the trajectory of the first one. In contrast, in previous work [4], a trajectory-based strategy has been proposed relying on nonlinear control techniques: lateral and longitudinal control are exactly decoupled, so that lateral guidance of each vehicle with respect to the same reference path can be achieved independently from longitudinal control, designed to maintain a pre-specified curvilinear vehicle inter-distance.

Fig. 1. Experimental vehicles: a RobuCab leading two Cycab

The potentialities of this last control approach have been demonstrated with the experimental vehicles shown in Fig.1 relying, as a first step, on RTK-GPS receivers for vehicle localization [4]. These sensors are however not reliable in urban applications, since satellite signals can be masked by tall buildings. Cameras appear as more appropriate, since the buildings offer a rich environment from an image processing point of view (in addition, they are definitely cheaper). Accurate absolute localization can indeed be obtained from monocular vision, relying on a structure from motion approach, but it is then expressed in a virtual vision world, roughly related to the actual metric one via a scale factor. Alas, this scale factor is not perfectly constant, so that the vision world appears slightly distorted with respect to the metric one. This alters noticeably the estimation of inter-vehicle distances, and therefore impairs longitudinal control performances. In previous work [1] and [2], it has been shown that such a distortion can accurately be corrected on-line in different ways, leading to satisfactory longitudinal performances. In the first one, direct distance between two successive vehicles is evaluated using telemetric information and makes it possible to optimize iteratively the correction during the motion. In the second approach same corrections are provided by a nonlinear observer based on odometric data and running on the lead vehicle. These approaches have here been refined and a comparative study is carried out to exhibit the advantages of each ones.

This paper is organized as follows: the platooning control strategy is first sketched in Section II. Then, absolute localization from monocular vision is discussed in Section III and a reference method to off-line optimize correction of the visual world is emphasized. Next, in Section IV, robustness and noise sensitivity of both on-line strategies is quantified during simulation test beds. Finally, experiments reported in Section V describe their behaviour in real conditions.

II. Global decentralized control strategy

A. Modeling assumptions

Urban vehicles involved in platooning applications are supposed to move at quite low speed (less than $5 m.s^{-1}$) on asphalted roads. Dynamic effects can therefore be neglected and a kinematic model can satisfactorily describe their behavior, as corroborated by extensive tests performed with our experimental vehicles shown in Fig. 1. In this paper, the kinematic tricycle model is considered: the two actual front wheels are replaced by a unique virtual wheel located at the mid-distance between the actual wheels. The notation is illustrated in Fig. 2.

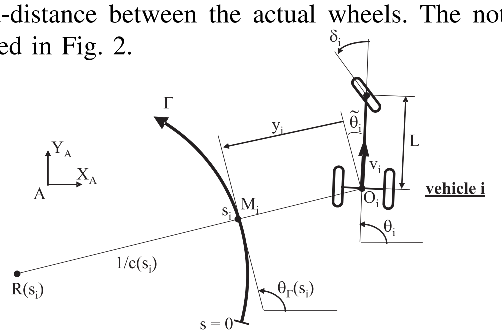

Fig. 2. Tricycle model description

- Γ is the common reference path for any vehicle, defined in an absolute frame $[A, X_A, Y_A]$.
- O_i is the center of the i^{th} vehicle rear axle.
- M_i is the closest point to O_i on Γ.
- s_i is the arc-length coordinate of M_i along Γ.
- $c(s_i)$ is the curvature of path Γ at M_i, and $\theta_\Gamma(s_i)$ is the orientation of the tangent to Γ at M_i w.r.t. $[A, X_A, Y_A]$.
- θ_i is the heading of i^{th} vehicle w.r.t. $[A, X_A, Y_A]$.
- $\tilde{\theta}_i = \theta_i - \theta_\Gamma(s_i)$ is the angular deviation of the i^{th} vehicle w.r.t. Γ.
- y_i is the lateral deviation of the i^{th} vehicle w.r.t. Γ.
- δ_i is the i^{th} vehicle front wheel steering angle.
- L is the vehicle wheelbase.
- v_i is the i^{th} vehicle linear velocity at point O_i.

B. Vehicle state space model

The configuration of the i^{th} vehicle can be described without ambiguity by the state vector $(s_i,\, y_i,\, \tilde{\theta}_i)$. The current values of these variables can be inferred on-line by comparing vehicle absolute localization to the reference path. It can then be shown (see [10]) that tricycle state space model is:

$$\begin{cases} \dot{s}_i = v_i \, \frac{\cos\tilde{\theta}_i}{1 - y_i \, c(s_i)} \\ \dot{y}_i = v_i \, \sin\tilde{\theta}_i \\ \dot{\tilde{\theta}}_i = v_i \left(\frac{\tan\delta_i}{L} - \frac{c(s_i)\, \cos\tilde{\theta}_i}{1 - y_i \, c(s_i)} \right) \end{cases} \tag{1}$$

Platooning objectives can then be described as ensuring the convergence of y_i and $\tilde{\theta}_i$ to zero, by means of δ_i, and maintaining the gap between two successive vehicles to a fixed value $d^\star$, by means of v_i. It is considered that $y_i \neq \frac{1}{c(s_i)}$ (i.e. vehicles are never on the reference path curvature center). In practical situations, if the l vehicles are well initialized, this singularity is never encountered.

C. Control law design

In previous work [4], it has been shown that exact linearization techniques offer a relevant framework to address platoon control: equations (1), as most of kinematic models of mobile robots, can be converted in an exact way into a so-called chained form, see [10]. Such a conversion is attractive, since the structure of chained form equations allows to address independently lateral and longitudinal control.

Steering control laws δ_i can first be designed to achieve the lateral guidance of each vehicle within the platoon w.r.t. the common reference path Γ. In these control laws, v_i just appears as a free parameter. Since conversion of equations (1) into chained form is exact, all nonlinearities are explicitly taken into account. High tracking performances (accurate to within $\pm 5cm$ when relying on an RTK GPS sensor) can then be ensured, whatever initial errors or reference path curvature are. Details can be found in [11].

Control variables v_i can then be designed to achieve longitudinal control. In nominal situation, the objective for the i^{th} vehicle is to regulate $e_i^1 = s_1 - s_i - (i-1)\, d^\star$, i.e. the arc-length longitudinal error w.r.t. the leader. This control objective is attractive, since the location s_1 of the leader represents a common index for all the vehicles into the platoon, so that error accumulation and inherent oscillations can be avoided. In addition, since it is an arc-length error, this control objective remains consistent whatever the reference path curvature is (in contrast with euclidian inter-distances). Nevertheless, for obvious safety reasons, the location of the preceding vehicle cannot be ignored. Therefore, in previous work [4], the longitudinal control law has been designed to control a composite error: a smooth commutation function gives the predominance either to the global error e_i^1 or to the local one $e_i^{i-1} = s_{i-1} - s_i - d^\star$ according to some security distance. Once more, exact linearization techniques have been used, so that nonlinearities in equations (1) are still explicitly accounted, ensuring high accurate regulation. More details, as well as experiment results carried out with Cycab and RobuCab vehicles (see Fig. 1), relying on RTK GPS sensors for vehicle localization and WiFi technology for inter-vehicle communications, can be found in [4].

III. Localization with monocular vision

The implementation of the platooning control laws presented in previous section requires that some sensors can provide each vehicle with its absolute localization, in a common reference frame (in order that the composite errors could be evaluated). RTK GPS receivers can supply such a localization, with a very high accuracy ($\pm 2cm$). They have successively been used in [4]. However, they are quite expensive sensors, and above all they are not appropriate to urban environments, since satellite signals are likely to be frequently masked by tall buildings. In previous work [8], absolute localization from monocular vision has been alternatively proposed, and satisfactory accurate lateral guidance of a sole vehicle along a given reference path has been demonstrated. An overview of the localization approach is sketched in Section III-A, and its limitations with respect to platooning applications are discussed in Section III-B.

A. Localization overview

The localization algorithm relies on two steps.

First, the vehicle is driven manually along the desired trajectory and a monocular video sequence is recorded with the on-board camera. From this sequence, a 3D reconstruction of the environment in the vicinity of the trajectory is computed. Because only one camera is used, this is a structure from motion problem well-known in the computer vision community. The computation of the reconstruction is done off-line with a method relying on bundle adjustment. The trajectory is thus referred in a non-metric virtual vision world. However, the total covered distance supplied by on-board odometers, when compared to the same quantity evaluated from vision algorithms, enables to propose a global scale factor such that this virtual vision world is nevertheless close to the actual metric world.

The second step is the real time localization process. Interest points are detected in the current image. These features are matched with the features stored in the visual memory as part of the 3D reconstruction. From the correspondences between 2D points in the current frame and 3D points in the visual memory, the complete pose (6 degrees of freedom) of the camera is computed. Then, the pose of the vehicle on the ground plane is deduced, and finally the vehicle state vector $(s_i, y_i, \tilde{\theta}_i)$ and the curvature $c(s_i)$ required in control laws can all be inferred. More details and localization performances can be found in [9].

B. Distortion in the virtual vision world

Platoon control in urban environment requires vehicle localization to be accurate to within some centimeters. The global scale factor computed from odometric data cannot guarantee such an accuracy: first, odometers cannot supply a covered distance accurate to within some centimeters when the reference trajectory length comes up to few hundred meters. Secondly, the distortion between the two worlds is alas varying along the trajectory. These limitations are illustrated in Fig.3: when the vehicle was moving, its trajectory has been recorded from monocular vision and from an RTK-GPS sensor. The distortion between the virtual vision world and the actual metric one appears clearly in the inserted plot in Fig.3 since the two trajectories do not properly fit, despite the global scale factor correction. In order to investigate further the discrepancy between the two worlds, the error between the covered arc-length distances computed from monocular vision and from RTK-GPS data is reported as the main plot in Fig.3. It can be noticed that, on one hand the drift in odometric measurement does not allow a proper evaluation of the global scale factor, so that the total arc-length distance is erroneous in the vision world (the error is $1.72m$, although the trajectory is only $115m$-long), and on the other hand the distortion between the two worlds is largely varying, since the error comes up to $7.48m$ in the mid-part of the trajectory.

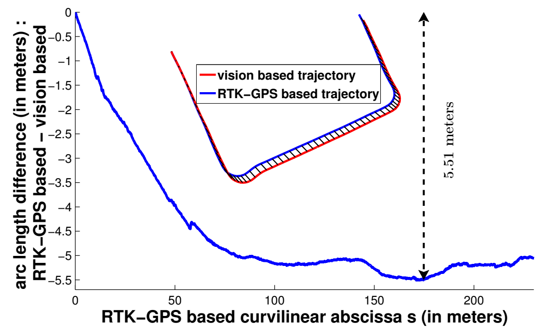

Fig. 3. Error in arc-length distance estimation with vision

These distorsions in the virtual vision world are not a concern as long as only lateral guidance is considered: since the sign of the lateral and angular deviations y_i and $\tilde{\theta}_i$ supplied by vision algorithms is always correct, these distorsions act only as control gain modifications. Asymptotic convergence of y_i and $\tilde{\theta}_i$ to 0 is therefore always guaranteed, and very satisfactory path following results can be obtained, as reported in [8].

The situation is different when longitudinal control is addressed: the distortions in the virtual vision world lead to inaccurate inter-vehicle distance evaluation, and therefore poor longitudinal control performances with respect to the metric world. In order to analyse the repeatability of such distorsions, lateral guidance along the $230m$-long trajectory shown in Fig.3 has been carried out with several vehicles and with different cameras. For each trial, local scale factors ensuring consistency between vision and actual distance along the trajectory have been optimized off-line according the following process:

The vision trajectory Γ^v is first divided into small parts $\Gamma^v_{\lambda_j}$ *(of size* $\Delta s^v_{\lambda_j} = \int_{\Gamma^v_{\lambda_j}} ds^v$*).* A set of actual arc-length measurements Δs_k, supplied by an RTK-GPS sensor, and the corresponding ones Δs^v_k, obtained by monocular vision, defined as:

$$\Delta s^v_k = \sum_{j \in J_k} \Delta s^v_{\lambda_j} \tag{2}$$

are then introduced, where the index set J_k targets trajectory parts covered by the k^{th} measurements Δs^v_k and Δs_k. Local scale factors λ_j, active on $\Gamma^v_{\lambda_j}$, are finally obtained using standard least square method by minimizing criterion (3) :

$$\sum_k \left(\Delta s_k - \sum_{j \in J_k} \lambda_j . \Delta s^v_{\lambda_j} \right)^2 \tag{3}$$

Two correction sets are reported in Fig.4. It can be observed that they present a very similar profile, and so do the other sets. As a conclusion, since distortions between the virtual vision world and the actual metric one are clearly repeatable, accurate longitudinal control relying solely on monocular vision appears attainable, provided that the set of local scale factor could be precisely estimated.

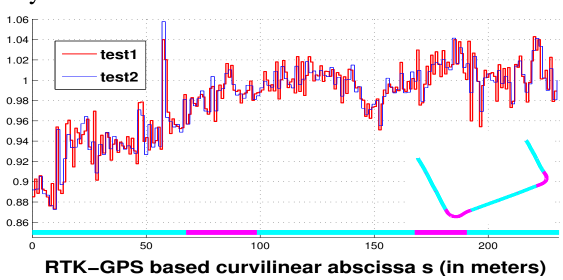

Fig. 4. Off-line local scale factor computation

IV. Curvilinear distance estimation

In the perspective of an on-line 3D reconstruction of the environment, simultaneously coupled with the localization, on-line correction strategies have been designed. Although RTK-GPS receivers prove to be efficient to scale vision data, they cannot be considered. On one hand they are not reliable in urban environments due to canyon effects, and on the other hand they are quite expensive when a large fleet of urban vehicles has to be equipped. Two alternative sensors have here been used: a laser rangefinder and odometers.

A. Local optimization from telemetric data

Local scale factors are here derived from the telemetric data supplied by a unique laser rangefinder. Some notations from the off-line strategy are here re-used:

(i) Vision and actual measurements Δs^v_k and Δs_k are here euclidian distances. Measurements Δs_k are supplied by the laser rangefinder of the 2^{nd} vehicle tracking the leader one.

(ii) To simplify notations, it is assumed that the correction set λ_j, computed along parts Γ_{λ_j} of the vision trajectory, also satisfies relation (2).

In contrast, the optimization is done according to a local criterion. When the $j-1^{th}$ part $\Gamma_{\lambda_{j-1}}$ has just been passed by the second vehicle, j^{th} correction λ_j is computed from the recorded sets of actual and vision measurements intersecting Γ_{λ_j}. The correction is first viewed as a polynomial $\lambda(s^v)$ of degree 2, obtained minimizing criterion (4).

$$\sum_k \left(\Delta s_k - \int_{\Gamma^v_k} \lambda(s^v) ds^v \right)^2, \text{ where } \Gamma^v_k = \bigcup_{j \in J_k} \Gamma_{\lambda^v_j} \tag{4}$$

The local correction λ_j is then computed as the average of the polynomial $\lambda(s^v)$ along part $\Gamma_{\lambda^v_j}$:

$$\lambda_j = (\Delta s^v_{\lambda_j})^{-1} \int_{\Gamma_{\lambda^v_j}} \lambda(s^v) ds^v \tag{5}$$

B. Observer design from odometric data

In this approach, the reference measurement in the metric world to be used to infer local scale factors is the vehicle linear velocity v_i supplied by the odometers. In the sequel, let us denote $(s^v_i, y^v_i, \tilde{\theta}^v_i)$ and $c^v(s^v_i)$ the i^{th} vehicle state vector and reference path curvature at s^v_i expressed in the virtual vision world. In view of the reference measurement to be used, a relevant way to describe the local scale factor at curvilinear abscissa s^v_i is the function:

$$\lambda(s^v_i) = \dot{s}_i \,/\, \dot{s}^v_i \tag{6}$$

It has been shown in [2] that the vehicle motion can be described from the variables actually available, i.e. the vehicle localization in the vision world and its linear velocity in the metric world. The arc-length evolution, expressed in the virtual vision world, thus follows :

$$\dot{s}^v_i = \frac{v_i . \cos \tilde{\theta}^v_i}{\lambda(s^v_i).(1 - y^v_i\, c^v(s^v_i))} \tag{7}$$

An observation model has then been designed in [2], relying on the duality between control and observation, from (7) :

$$\dot{\hat{s}}^v_i = \frac{v_i . \cos \tilde{\theta}^v_i}{u_i.(1 - y^v_i\, c^v(s^v_i))} \tag{8}$$

with $\hat{s}^v_i$ the observed curvilinear abscissa in the virtual vision world and u_i the control variable. In order to be representative of the local scale factor $\lambda(s^v_i)$, the control variable u_i is designed such that the observed state $\hat{s}^v_i$ converges with the measured one s^v_i as follows :

$$u_i = \frac{v_i . \cos \tilde{\theta}^v_i}{(\dot{s}^v_i - K.\epsilon)(1 - y^v_i . c^v(s^v_i))}, \text{ with } \begin{cases} \epsilon = (\hat{s}^v_i - s^v_i) \\ K > 0 \end{cases} \tag{9}$$

Injecting (9) into (8) indeed leads to : $\dot{\epsilon} = -K \cdot \epsilon$. Variable u_i can then be regarded as an accurate estimation of the local scale factor at the curvilinear abscissa s^v_i. Providing that it is properly initialized, it also proposes no singularity (see [2]).

C. Simulations

In this section, simulation results are presented to compare on-line correction methods and investigate the sensitivity to their main parameters. In order to be representative of actual conditions, simulation test beds have been run with the following parameters, tuned in order to be representative of actual conditions:

- Scale factors and reference trajectory shown on Fig. 4 have been selected.
- Visual data are provided with a $15Hz$ sampling frequency and two standard deviations $\sigma_v = 0m$ and $\sigma_v = 0.02m$ have been considered.
- Two standard deviations $\sigma_t = 0m$ and $\sigma_t = 0.01m$ of telemetric data have also been considered.
- Standard deviation of odometry is $\sigma_o = 0.015m.s^{-1}$.

Local optimization from telemetric data: the most significant results are recorded in Fig. 5 according to influential parameters, namely the platoon velocity v_1 (= the leader velocity), the desired inter-vehicle gap $d^\star$, and the approximative arc-length of corrected parts Δs_λ. The error between estimated and simulated arc-length distances has been quantified along trajectory parts of different sizes: 5m, 10m and 40m. As the observed results are within the same range and reflect the same trends, averaged error on only the 5m-length parts has been recorded in Fig. 5.

v_1 (m.s^{-1})	$d^\star$ (m)	Δs_λ (m)	average error (10^{-3}m) $\sigma_v = 0m$, $\sigma_t = 0m$	$= 0.02m$, $= 0.01m$
0.5	2	0.1	0.0769	4.0296
1	2	0.1	0.0767	5.4979
3	2	0.1	0.0847	8.1975
1	5	0.1	1.0057	3.0993
1	7	0.1	2.0748	2.8135
1	5	2	1.4577	2.4323

Fig. 5. Influence of parameters on local optimization performances

First, since vehicle velocity has to be bounded in urban areas, tests have been limited to $v_1 < 3$m.s^{-1}. Values show clearly that this parameter do not impact approximation results if perfect data (without noise) are supplied. In contrast, when noise is added, a low speed is preferable since the number of measurements considered in criterion (4) is more important thus decreasing noise disturbances. Next, in order for the second vehicle to properly track its preceding one in safe conditions, $d^\star$ is chosen in interval $[2; 7]$. Low values ensure that polynomial $\lambda(s^v)$ is estimated on a short distance, reflecting properly the actual scale factor in case of perfect data. Since higher values minimize in criterion (4) the magnitude of noise related to telemetric measurements, trend is reversed with noisy data. Finally, last parameter is logically chosen such that $\Delta s_\lambda < d^\star$. It represents the interval on which polynomial $\lambda(s^v)$ is averaged, and consequently small values are more beneficial without noise. If we consider noise, smoother results are obtained with higher values, but improvement is very slight, especially for high $d^\star$ values.

Observer design from odometric data: for comparison purposes, results recorded in Fig. 6 are evaluated just as for previous simulation test beds and first influential parameter v_1 is investigated in the same range. Values of gain K are investigated in interval $[0.5; 5]$.

v_1 (m.s^{-1})	K	average error (10^{-3}m) $\sigma_v = 0m$, $\sigma_o = 0m.s^{-1}$	$= 0.02m$, $= 0.015m.s^{-1}$
0.5	0.5	0.1974	8.4819
1	0.5	0.4176	8.7286
3	0.5	1.4615	12.4672
1	2	0.3905	11.6021
1	5	0.3892	13.0619
3	2	1.2271	12.2550

Fig. 6. Influence of parameters on observer performances

It can be noticed that performances are impaired when velocity v_1 is high. In that case the length of corrected parts, that linearly depends on v_1, reaches larger values and the observer delay damages scale factor estimation. Next, focusing on performances with perfect data, faster convergence is achieved with higher gain values K. It unfortunately leads to oscillations when noise is considered and preceding remark is no more correct.

To conclude these test beds, it is to notice that both strategies present very satisfactory results. With respect to accuracy, the telemetric based approach is more efficient, see Fig. 5 and 6. The observer based strategy however presents attractive aspects. Associated algorithm runs whatever v_1 value, while a large $d^\star$ value is necessary for the telemetric based approach to achieve the numerical approximation when v_1 value is high. From a practical point of view, the observer strategy is also more convenient. First, combining telemetric and visual data is quite intricate, and secondly a tracking algorithm is required. The platoon communication scheme is finally complicated since the second vehicle has to broadcast corrections to the whole platoon.

V. Experimental results

In order to investigate the capabilities of the proposed approach, several experiments have been carried out with three vehicles at Campus des Cézeaux, in Clermont-Ferrand.

1) Experimental set-up: The experimental vehicles are shown in Fig. 1. They are electric vehicles, powered by lead-acid batteries providing 2 hours autonomy. Two *(resp. four)* passengers can travel aboard the Cycab *(resp. the RobuCab)*. Their small dimensions (length 1.90m, width 1.20m) and their maximum speed (5m.s^{-1}) are appropriate to urban environments. Vehicle localization algorithms and platoon control laws are implemented in C++ language on Pentium based computers using RTAI-Linux OS. Laser rangefinders provide telemetric data at a 60Hz sampling frequency, with a standard deviation within 2cm. The cameras supply visual data at a sampling frequency between 8 and 15*Hz*, according to the luminosity. The inter-vehicle communication is ensured via WiFi technology. Since the data of each vehicle are transmitted as soon as the localization step is completed, the communication frequency is similar to the camera one. Finally, each vehicle is also equipped with an RTK-GPS receiver, devoted exclusively to performance analysis: its information are not used to control the vehicles.

2) Experimental results: The experiment reported below consists in platoon control, with three vehicles, along the $230m$-long reference trajectory shown in Fig. 3. The local scale factors computed on-line from odometric data by the leader vehicle (with $K = 0.5$ and $v_1 = 1m.s^{-1}$) are shown in green in Fig. 7. The ones obtained off-line as well as those computed on-line from telemetric data (with $d^\star = 5m$ and $\Delta s_\lambda = 0.1$) and retransmitted by the second vehicle are respectively reported in red and blue in Fig. 7. It can be noticed that both scale factors sets computed on-line are very close to the actual ones evaluated off-line from RTK-GPS measurements.

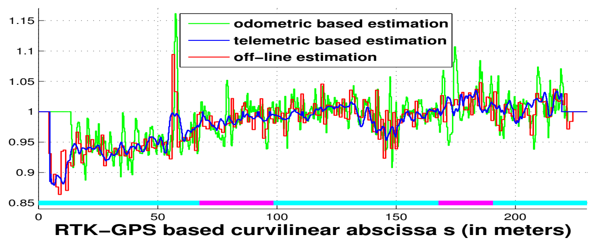

Fig. 7. On-line scale factor estimation

Finally, platoon control performances are evaluated in Fig. 8, according the correction applied on the trajectory. At the top are presented the second vehicle results and the third ones figure at the bottom. When inter-distance error is directly deduced from raw localization vision data, longitudinal control is largely erroneous, as shows the black curve in Fig. 8. These large errors, namely $40cm$ for the second vehicle and $70cm$ for the third one, show clearly the significance and the relevance of local corrections. As expected, best corrections are provided off-line: the longitudinal errors are as accurate as previously when RTK-GPS data were used (see [4]) to control the vehicles. Whatever the vehicle, they indeed satisfactorily remain within $10cm$. When on-line corrections are provided, same control performances are maintained for the second vehicle while those of the third one are slightly depreciated during the abrupt scale factor variation ($s_1 \in [60, 80]m$). Nevertheless, the inter-distance errors do not exceed $16cm$ and $21cm$, respectively with observer (9) and local optimization (4).

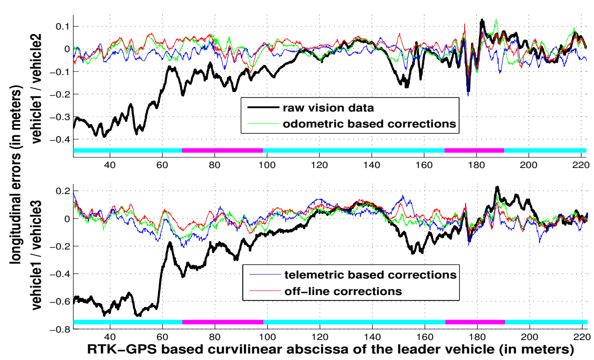

Fig. 8. Vehicle inter-distance errors

VI. Conclusion

In this paper, vehicle platooning in urban environments has been addressed. First, a global decentralized control strategy, taking advantage of inter-vehicle communications, has been proposed, in order to avoid error accumulation inherent to local control approaches.

Vehicle absolute localization has been derived from an on-board camera and two approaches have been proposed to on-line estimate local distortion between actual and virtual vision worlds: first, a local optimization technique, relying on vehicle inter-distances measured with a laser rangefinder, and secondly a nonlinear observer supported by odometric data.

The capabilities of the two approaches have been investigated and compared, via exhaustive numerical simulations. Then full-experiments, carried out with three vehicles have finally demonstrated the efficiency of the proposed approaches. Further experiments, involving vehicles led by a manually guided vehicle have to be conducted to emphasize the benefits of on-line corrections when the reference trajectory is being created.

References

[1] P. Avanzini, E. Royer, B. Thuilot, and P. Martinet. A global decentralized control strategy for urban vehicle platooning using monocular vision and a laser rangefinder. In *IEEE Intern. Conf. on Control, Automation, Robotics and Vision (ICARCV)*, Hanoi (Vietnam), 2008.

[2] P. Avanzini, B. Thuilot, E. Royer, and P. Martinet. A global decentralized control strategy for urban vehicle platooning relying solely on monocular vision. In *ICRA, International Workshop on Robotics and Intelligent Transportation System (RITS10)*, Anchorage (Alaska), 2010.

[3] S. Benhimane and E. Malis. Vision-based control for car platooning using homography decomposition. In *IEEE Intern. Conf. on Robotics and Automation (ICRA)*, pages 2173–2178, Barcelona (Spain), 2005.

[4] J. Bom, B. Thuilot, F. Marmoiton, and P. Martinet. A global strategy fo urban vehicles platooning relying on nonlinear decoupling laws. In *IEEE Intern. Conf. on Intelligent Robots and Systems (IROS)*, pages 1995–2000, Edmonton (Canada), 2005.

[5] R.E. Caicedo, J. Valasek, and J.L. Junkins. Preliminary results of one-dimensional vehicle formation control using structural analogy. In *American Control Conference (ACC)*, Denver (USA), 2003.

[6] L. Consolini, F. Morbidi, D. Prattichizzo, and M. Tosques. Leader-follower formation control of nonholonomic mobile robots with input constraints. *Automatica*, 44(5):1343–1349, 2008.

[7] W. Dong and Y. Guo. *Formation Control of Nonholonomic Mobile Robots Using Graph Theoretical Methods*, chapter in Cooperative Systems, Springer Verlag LNEMS series n°588, pages 369–386. 2007.

[8] E. Royer, J. Bom, M. Dhome, B. Thuilot, M. Lhuillier, and F. Marmoiton. Outdoor autonomous navigation using monocular vision. In *IEEE Intern. Conf. on Intelligent Robots and Systems (IROS)*, pages 3395–3400, Edmonton (Canada), 2005.

[9] E. Royer, M. Lhuillier, M. Dhome, and T. Chateau. Localization in urban environments : monocular vision compared to a differential GPS sensor. In *Intern. Conf. on Computer Vision and Pattern Recognition (CVPR)*, pages 114–121, San Diego (USA), 2005.

[10] C. Samson. Control of chained systems: application to path following and time-varying point stabilization of mobile robots. *IEEE Trans. on Automatic Control*, 40(1):64–77, 1995.

[11] B. Thuilot, J. Bom, F. Marmoiton, and P. Martinet. Accurate automatic guidance of an urban electric vehicle relying on a kinematic GPS sensor. In *IFAC Symposium on Intelligent Autonomous Vehicles (IAV)*, Lisbon (Portugal), 2004.

[12] D. Wang and M. Pham. *Unified control design for autonomous car-like vehicle tracking maneuvers*, chapter 8 in “Autonomous Mobile Robots: sensing, control decision-making and applications”, pages 295–329. CRC Press, 2006.

[13] S.Y. Yi and K.T. Chong. Impedance control for a vehicle platoon system. *Mechatronics*, 15(5):627–638, 2005.